# Dynamic Model of Lignin Growing in Restricted Spaces

**Marc R. Roussel**†

*Department of Chemistry, University of Toronto, Toronto, Ontario, Canada M5S 1A1*

**Carmay Lim***,‡

*Protein Engineering Network of Centres of Excellence and Departments of Molecular and Medical Genetics, Biochemistry, and Chemistry, University of Toronto, MSB 4388, 1 King's College Circle, Toronto, Ontario, Canada M5S 1A8*

*Received July 8, 1994*®

ABSTRACT: A discrete, dynamic model of lignification most suited to studying lignin growing in highly restricted spaces is presented. This model satisfactorily reproduces many known properties of lignin. It is argued that the model therefore produces spatially realistic structures for lignin. The effects of hemicellulose binding on lignification are studied. It is shown that the geometry of the hemicellulose matrix is an important factor in determining the magnitude of these effects.

## 1. Introduction

Understanding lignin is a pressing technological and scientific problem. On the one hand, lignin gives wood much of its strength[1] and is a promising source of new polymeric materials.[2,3] On the other hand, it colors pulp and makes bleaching necessary.[4]

Despite its importance, there are significant gaps in our understanding of lignin. Even such fundamental questions as the degree of organization of native lignin remain controversial: Lignin has traditionally been considered to be a random network, a view for which there is considerable experimental evidence.[5,6] However, it is now clear that other structural components of wood exert a significant organizing influence on lignin deposition.[7] Nevertheless there may be a significant random component in the polymerization process. There are also theoretical arguments for nonrandom lignin structures[8] relying implicitly on the assumption that lignin deposition is thermodynamically rather than kinetically controlled. At this point, it is impossible to say whether this is generally true. Goring's suggestion that lignins from different sources may be fundamentally morphologically different seems sensible, given the conflicting evidence.[5] Random models of lignin thus continue to be of some interest.

In vivo, lignin is formed by the dehydrogenative polymerization of 3-(4-hydroxyphenyl)-2-propen-1-ol (*p*-coumaryl alcohol, structure **1**,

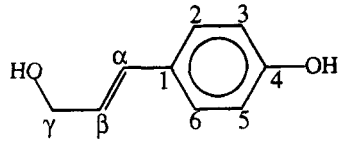


shown with the numbering scheme standard in works on lignin[9]) and its derivatives 3-(3-methoxy-4-hydroxyphenyl)-2-propen-1-ol (coniferyl alcohol) and 3-(3,5-dimethoxy-4-hydroxyphenyl)-2-propen-1-ol (sinapyl alcohol);[1,4,10] collectively, these units are known as monolignols.[9] (The monolignols are present in different ratios according to both the species and tissue studied.[4,11]) The complexity of lignin is largely due to the number of resonance structures of phenylpropane radicals: For instance, the coniferyl alcohol radical has five resonance structures, of which four are thermodynamically significant.[12] The monolignols are present in limited quantities during lignification so that, to a good approximation, a few dilignols are initially formed, with further polymerization consisting primarily of addition of monolignols to the initially formed polymeric centers.[1,4,13]

As most lignin is closely associated to carbohydrates, in particular to hemicellulose in woody tissues,[1,4,14] it is quite difficult to extract a chemically unmodified, carbohydrate-free lignin fraction from wood.[4] Furthermore, it may be that lignin−carbohydrate complexes, collectively known as glycolignins,[14] are partly responsible for pulp discoloration[15] so that these complexes are themselves interesting objects of study.

As a result of the complexity of lignin, computer modeling has played an important role in the development of the field. There are two complementary approaches to lignin modeling: quantum chemical calculations on small polymers[8,16,17] and simulation of the formation of a large polymer. Our work falls in the latter category, which we briefly review. In the pioneering work of Glasser and co-workers,[18−24] monolignols are added one at a time to the growing polymer; reactions are accepted or rejected both on the basis of input parameters (monolignol radical reactivities, bond distribution, etc.) and according to the evolving statistical properties of the simulated polymer. Essentially, the intrinsic chemistry of the monolignols is modified during the simulation in order to reconcile the model to experimental data. In the model of Lange and coworkers,[25,26] based in part on the Flory−Stockmayer treatment of lignin by Bolker and Brenner,[27] lignification is viewed as a stepwise process: First, dilignols are formed which then oligomerize into chains, and finally the chains form cross-links. There is some experimental support for this view of lignification, but it is unclear whether occasional random deviations from this scenario (e.g., early formation of polymer branch points) play a role in the overall structure of the polymer. In Jurasek's model,[28] a determined effort is made to construct realistic lignin structures in space by taking careful account of the size and geometry of the monolignols as they are added to the polymer. Each of these models proceeds from a particular view of the lignifi-

† Present address: Centre for Nonlinear Dynamics, McGill University, 3655 Drummond Street, Montreal, Quebec, Canada H3G 1Y6.

‡ Present address: Institute of Biomedical Sciences, Academia Sinica, Taipei 11529, Taiwan, Republic of China.

® Abstract published in *Advance ACS Abstracts,* November 15, 1994.

0024-9297/95/2228-0370$09.00/0 

cation process to an implementation in the form of a sequentially executed program. Although this class of models seems to be particularly effective in detecting stoichiometric anomalies in experimental data,[20] it is not clear that they necessarily produce realistic spatial structures for the lignin polymer.

In contrast to the studies outlined above, we have attempted to capture the dynamics of lignification by establishing some simple transport and bonding rules and allowing these to run their course. The "physics" of the model is fixed at the outset and mimics in vivo physics, including the "parallelism" resulting from the simultaneous presence of many molecules in the reaction space. In other words, we attempt to recreate the *conditions* of the reaction rather than attempt to generate the products directly.

In previous work,[29] we described a novel approach to modeling the dynamics of polymerization leading to realistic structures for macromolecules of very high molecular weight. The methods developed were applied to a "diatomic" model of lignin. In section 2, we describe a minimal model of lignin in the plane (most appropriate to modeling lignin growing in restricted spaces) based on the methods introduced in our earlier work. Enhancements introduced here include both lignin–hemicellulose complexes and a refined treatment of branching. On the basis of our results (section 3), we feel that the current model captures the essential features of in vivo lignification.

## 2. Computational Methods

We have chosen to apply discrete simulation methods for efficiency and simplicity. Both time and space are discretized; in particular, space is represented by a square grid of 256 × 256 cells with periodic boundary conditions. (While we will loosely refer to this arrangement as a plane, the boundary conditions make it a torus.) Planar models such as these are best suited to modeling lignin growing in restricted spaces such as the secondary wall of a wood fiber. (Note that the order observed in secondary wall lignin occurs at the mesoscopic level, not at the microscopic.[30] Also, while it might be tempting to associate planar models with lignin monolayers,[31] this would be wrong since monolayers are produced by spreading *bulk* lignin on an interface rather than by growing a polymer there.) Furthermore, we have opted to use purely local rules to control the polymerization process; the reactivity of the monolignol radicals makes this a reasonable model feature.[6]

At every time step, a coordinate origin is randomly selected and the plane is cut up into 2 × 2 blocks of cells. (This is a Margolus partitioning.[32]) Over time, the random origin selection insures that all different partitions are sampled. There are three types of "moves" in these blocks: influx, diffusion, and bonding. Influx is the addition of monomer radicals to the reaction space; in vivo, this would correspond to a combination of the synthesis, release, and catalytic dehydrogenation of monolignols by plant cells. In this simple model, only the monomers diffuse; once a dilignol (or higher oligomer) has formed, it is fixed in space. (It is known that diffusion-limited aggregation models are insensitive to the oligomer diffusion constant, provided that this is lower than the monomer diffusion constant. In particular, it seems not to matter if the oligomers do not diffuse at all.[33]) Finally, some rules must be provided for bonding monolignols to monolignols and monolignols to oligomers. (Oligomers do not, in this model, directly bond to one another because they cannot diffuse into proximity. Rather, they are bridged by monolignols when they grow sufficiently close to one another.) Bonds are formed combinatorially by joining loci on adjacent molecules. This maximizes the number of bonds considered, while minimizing the complexity of the model. All of the rules are executed in parallel.

The implementation architecture for this model is a cellular automata machine (CAM).[32] The principal advantages of this modeling environment are speed and ease of programming.[29] On the other hand, designing models using more than four bit-planes is awkward. Since Monte Carlo simulation of the sort we propose requires one bit-plane for random number generation, this effectively limits models to three bits of state information; i.e., only eight states are available, of which one must be set aside to represent empty space.

Given the limited number of states and the desire to incorporate hemicellulose and branching, each monolignol is represented by a point. Three bonding sites are considered, namely, O-4, C-$\beta$, and C-5 (numbering scheme as in structure **1**); roughly 75% of the bonds in native lignin can thus be formed combinatorially. To keep the state space small, in addition to permitting only bonds for which there is experimental evidence, the assumption is made that C-5 cannot be bound unless O-4 already is. (This allows the state of any cell in the simulation to be held in three bits, given the desire to represent hemicellulose.) A branch point is formed whenever all three sites on a single monolignol are bound. The slightly artificial bonding constraint described above favors the formation of a polymer backbone composed primarily of $\beta$-O-4 bonds with branching due mostly to other bond types, in accord with most common descriptions of the lignin polymer.[1]

Furthermore, one cell state is reserved for hemicellulose. C-$\beta$ to hemicellulose bonds are formed, but no accounting is done on the hemicellulosic side of the bond; i.e., a hemicellulose site is assumed to be capable of as many bonds as it makes contacts with lignin. (Relatively little is known about the structures of lignin–hemicellulose complexes. However, C-$\alpha$ to sugar bonds have been demonstrated in vitro.[1] Given the similarity in chemical properties of the C-$\alpha$ and C-$\beta$ sites, assuming that the latter can also form bonds to hemicellulose is reasonable.)

Briefly, the influx, diffusion, and bonding rules are as follows:

**Influx.** Every $n$th step, one quarter of the blocks are randomly selected. For every selected block, a single position (of the four available) is designated for influx. If this position is empty, a monolignol is added. Influx is turned off once the target surface density $\mathscr{D}^*$ is reached.

**Diffusion.** At every step, a random shuffle of each block is formed. If this shuffle leaves bonded monolignols undisturbed and conserves the number of monomers, it is executed. Combined with Margolus repartitioning, this produces diffusive movement.

**Bonding.** In each block, attempt to form bonds in the following order:

1. With probability $1/16$, attempt to form a bond between C-$\beta$ and hemicellulose.
2. Attempt to form a 5–5 bond.
3. Attempt to form a $\beta$–5 bond.
4. Attempt to form a 4–O-5 bond.
5. Attempt to form a $\beta$–O-4 bond.

6. Attempt to form a $\beta-\beta$ bond.

If the first type of bond cannot be formed (because the probabilistic test failed or because either or both of the required bonding partners is unavailable), try the next and so on until all possibilities have been exhausted.

Since position C-5 cannot be bound before O-4, this ordering of the bonds results in roughly the right proportion of each bond type, i.e., $\beta-$O-4 > 5$-$5 > $\beta-$5 > 4$-$O-5 > $\beta-\beta$; this sequence varies somewhat from one lignin source to another but can in any event easily be altered by reordering the bond attempts in the above list. The hemicellulose bonding probability was chosen capriciously, there being a dearth of experimental data on this subject.

The model incorporates a relaxation time $\tau$; when $\tau$ time steps pass without any new bonds being formed, the simulation is halted.

## 3. Results and Discussion

Recall that our model has three parameters: the relaxation time $\tau$, the target surface density $\mathscr{D}^*$, and the influx period $n$. The effects of these parameters on the model properties have been examined. As expected, since $\tau$ only serves to recognize a completed simulation, it has very little effect on the outcomes. On the other hand, both the density and the influx period have measurable effects on the model behavior.

The dependence of some of the model's properties on $\mathscr{D}^*$ and $n$ is not unexpected: The fractional degree of polymerization (DP; the number of bonds divided by the number of monomers) rises and the phenyl$-$OH content decreases with both $\mathscr{D}^*$ and $n$, the influx period, the latter result being in agreement with the outcomes of in vitro lignification experiments in which the rate of influx was varied.[34] The proportion of trifunctional (branch point) monolignols also varies with these parameters, rising with both $\mathscr{D}^*$ and $n$.

The influx period $n$ has a greater effect on the polymer morphology than might at first be suspected. This is due to the branching. At low $n$, the reaction space quickly becomes so crowded that almost every monolignol has several bonding opportunities at every time step, resulting in a very rapidly formed, uniform polymer with very few branch points.[34] For larger $n$ the polymer coagulates, forming a much larger number of branch points. Figure 1 illustrates these observations.

In addition, we studied the percolation behavior of the model.[35] Percolation theory has previously been used to understand the delignification process.[36] We identified the percolation threshold by plotting $f$, the ratio of the mass of the largest polymer formed to the total simulation mass, against $\mathscr{D}^*$; at the threshold, this fraction rises sharply.[35] The percolation threshold for our model occurs at $\mathscr{D}^* = 0.402$ when $n = 1000$ and $\tau = 100$. (The value of $n$ used is optimal, in a sense discussed below.) See Figure 2.

Alternatively, we can frame the percolation behavior in terms of polymer gelation theory; in this theory, the percolation threshold is called the gel point.[27,37-39] The gel point separates an initial period of increase in the mean molecular weight of the sol phase from a period of decrease.[37] Our results (Figure 3) are in qualitative agreement with standard gelation theory, even if the physical situation modeled is a little different in the two cases as the monomers are added gradually in our model rather than simply forming a static pool. Note also that this model and our previous diatomic model[29] produce very similar gelation curves when run with the same parameters. The main differences are the maximum sol phase molecular weight and the long-time limit: Both are higher in the diatomic model.

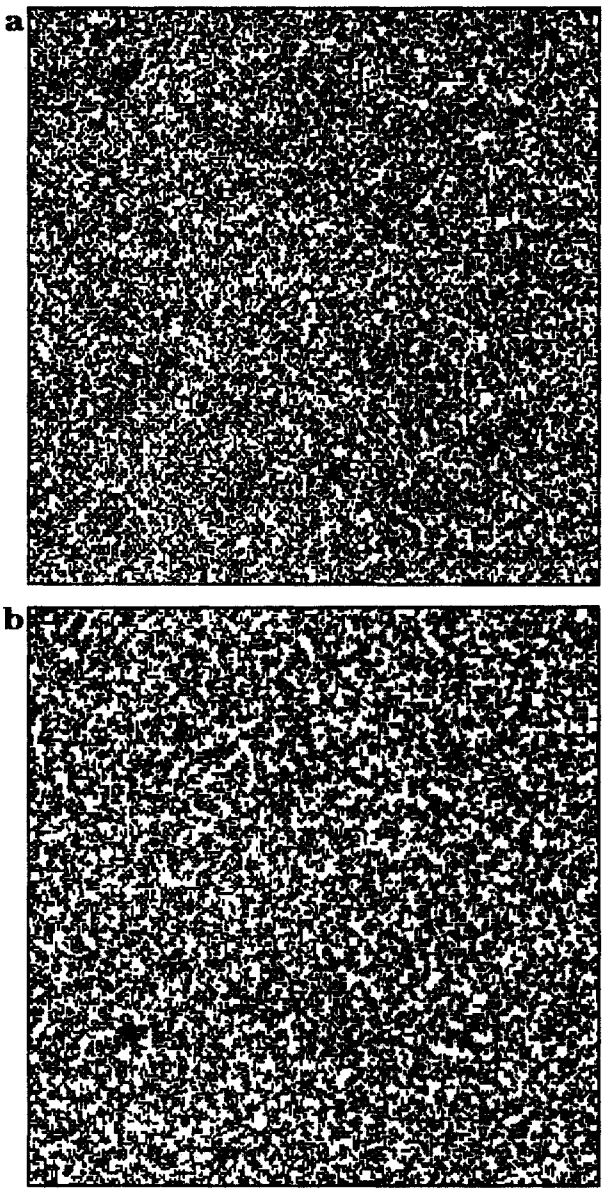


**Figure 1.** Model lignin polymer grown at (a) $n = 2$ and (b) 2000; in both cases $\tau = 100$ and $\mathscr{D}^* \approx 0.476$. Each pixel represents a monolignol, so each cell (occupied or not) represents a square of side about 4 Å; the simulation space is composed of 256 × 256 cells, corresponding therefore to a square physical space whose side is just over 1000 Å long. At larger values of $n$, the polymer is more highly coagulated. This is related to the branching: The fraction of trifunctional monomers rises from 6% to just under 20% as $n$ rises from 2 to 2000.

We can understand the percolation/gelation behavior of the model as that of a multicenter growth process.[40] Since, in our model, only monomers are subject to diffusion, after the establishment of a few small oligomers early in the simulation, most of the polymerization consists of addition of monomers to existing polymers. The mean radii of these polymers grow until, near the percolation threshold, they begin to merge. This causes rapid growth of the "gel" phase at the expense of the larger polymers in the "sol" phase as the latter are joined to the former, at first by single-monomer bridges but eventually by a complex network of cross-links. It

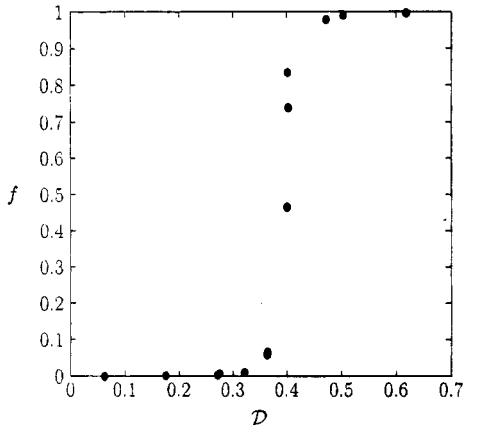


**Figure 2.** Percolation threshold determination for the lignin model. Each point represents a distinct realization of the model at $\tau = 100$ and $n = 1000$. $\mathscr{D}$ is the terminal density in each realization; $f$ is the ratio of the mass of the largest polymer formed to the total mass. $f$ rises sharply in the neighborhood of the percolation threshold.

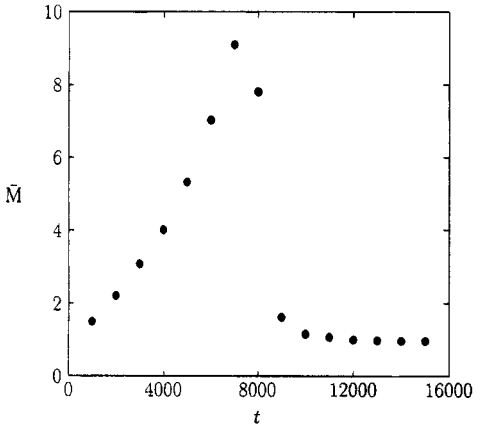


**Figure 3.** Time-dependent gelation graph for the lignin model. These points were obtained from time slices of a single realization of the model run with $\tau = 100$ and $n = 1000$. $\bar{M}$ is the number-average molecular weight of the sol phase (defined in our simulation as the collection of polymers obtained by removing the single largest one formed from the field, in units in which a single monomer has a weight of 1); the simulation time $t$ is in steps. The gel point occurs between 7000 and 8000 simulation steps, during which period $\mathscr{D} \in (0.397, 0.432)$, in accord with the percolation threshold determination of Figure 2. The mean molecular weight asymptotically approaches 1 at large simulation times as the number of large polymers not incorporated into the main body decreases to zero and the remaining unbound monomers become the only occupants of the sol phase.

should be understood that, although the *mean* molar weight in the sol phase near the gel point is under 10 (Figure 3), this is largely due to the presence of unreacted monomers (each of weight 1); in a typical realization, the sol-phase polymers near the gel point include several representatives in the 100–1000 weight range. It is the incorporation of these larger polymers in the gel phase which causes the mean molecular weight to crash. Figures 2 and 3 give the statistical behavior of the model; Figure 4 shows several frames of the detailed evolution.

In vivo, lignin grows to fill a space. Thus, in vivo conditions correspond to models run at densities above the percolation threshold; below this threshold, one cannot claim to be filling space in any reasonable sense. Furthermore, the rate of influx is low,[34] corresponding to large $n$ in our model. We therefore ran our model several times with the parameters $\mathscr{D}^* = 0.476$, $n = 1000$, and $\tau = 100$. The results are summarized and compared to experimental data from milled wood lignins in Table 1. Unfortunately, direct comparisons to native lignin data would be meaningless because the topological constraints of a planar model put the high degrees of polymerization of the native polymer completely out of reach.[41–47] Measurable properties of the model however do approach those of milled wood lignin, a substance related to the native polymer by rupture of a significant number of $\beta$–O-4 bonds. Even in this case, however, the planar constraints are such that perfect agreement is not possible. Reassuringly, the differences between the experimental and model data sets show precisely the expected relationship for related two- and three-dimensional systems: The fractional DP and the degree of branching should be lower and the phenyl–OH content higher in the two-dimensional system. (We conclude this by an argument similar to that used to determine that the percolation threshold of a two-dimensional model should be higher than that of a higher-dimensional model.[35])

**Table 1. Properties of the Lignin Model (Parameters $\mathscr{D}^* = 0.476$, $n = 1000$, and $\tau = 100$) Compared to Experiment[a]**

| | experiment | model |
|---|---|---|
| (bound C-$\beta$)/(bound O-4)[12,24] | 1.0–1.3 | 1.43 |
| (bound O-4)/(bound C-5)[12,24] | 1.2–4.8 | 2.33 |
| DP[4,12,24,50] | 0.95–1.06 | 0.869 |
| phenyl–OH %[4,12,24,50] | 17–35 | 39.2 |
| branch-point fraction[27] | 0.277 | 0.199 |

[a] The experimental values of the ratios of bound sites are computed on the basis of the relative abundances of only the five bond types considered in this model. DP is the fractional degree of polymerization, i.e., the number of bonds per monomer; phenyl–OH % is the percentage of free phenols; the branch-point fraction is the fraction of trifunctional monomers in the final polymer. The experimental values are from a variety of sources for milled wood lignins, as cited above. The model values are averages over 11 realizations for the given parameters.

We wish to emphasize that all the results collected in this paper indicate that we have been successful in our aim to model lignin in the plane. Thus, the structures shown in Figure 4 can be viewed as likely structures for lignin grown in highly restricted spaces but in the absence of significant interaction with carbohydrates. Much of the structure can be seen to resolve to dense "knots" connected by slender threads.

We now turn to a consideration of the effect of hemicellulose. We emphasize that this study will yield only qualitative information since the hemicellulose bonding probability used is a simple guess. We studied the effect of hemicellulose by growing lignin in a strip of width $w$ between two strips of hemicellulose, each of these strips extending the length of the simulation plane. (Because of the periodic boundary conditions, the two strips of hemicellulose, which were placed at the edges of the plane, are really just a single strip of width $256 - w$. The effect of this arrangement is to cut the torus in which the lignin is grown, reducing it to a cylinder of height $w$; each (circular) edge of the cylinder is lined with hemicellulose.)

The properties of the model are relatively insensitive to $w$ except at small values of this parameter: For small values of $w$, the fractional DP and degree of branching drop significantly, while the phenyl–OH content rises sharply. We now show that these results are a natural consequence of the geometry chosen. Consider a particular monolignol on the simulation plane. If this monolignol is away from the hemicellulose, it has eight neighbor sites to which it may attempt to form bonds.

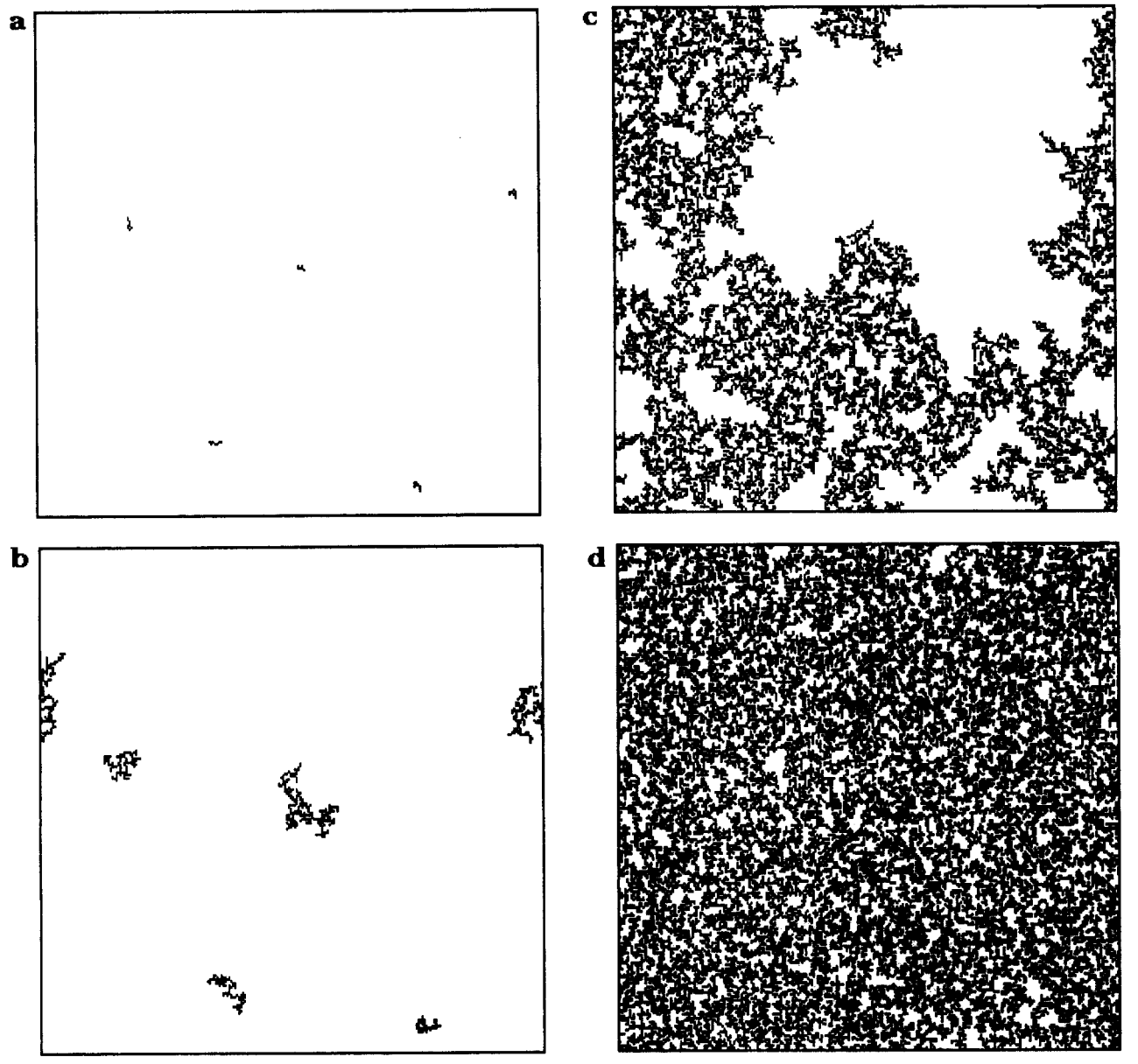


**Figure 4.** Time evolution of a few specific polymers, for the same realization of the model used to produce Figure 3, at (a) $t$ = 1002, (b) 6012, (c) 8016, and (d) 10020. Each pixel represents a monolignol. Note that, due to the periodic boundary conditions, polymers split across the boundaries are connected. This series of figures clearly shows the process whereby the growing polymers merge into each other as the percolation threshold is approached. While this is difficult to determine by eye, note that the time slice at $t$ = 8016 consists of three distinct polymers of masses 10587, 3693, and 299 (in monomer units); these polymers are clearly on the verge of merging into a greater mass at this point.

On the other hand, if the monolignol bonds to hemicellulose, because of the flatness of the interface and because only one lignin–hemicellulose bond is permitted per monomer, two of the hemicellulosic neighbors can only block the approach of other monolignols to the one anchored to the surface; worse, if a monolignol in contact with the hemicellulose reacts with another monolignol through its C-$\beta$ functionality, three neighbor sites are blocked. Thus, we expect the DP and degree of branching to drop and the phenyl–OH content to rise as the number of bonding opportunities at the hemicellulose interface is depressed. Accordingly, a rough lignin–hemicellulose interface with an average contact number of less than 3 should increase the DP of the model.

We verified this last bit of reasoning by comparing the bonding behavior of lignin grown in cylinders with two different hemicellulose wall geometries: the flat geometry and a regularly crenellated wall (Figure 5). There are various ways to measure the length of an interface; in our case, a sensible measure is the number of sites which touch the hemicellulose. Using any reasonable measure, however, the same result is obtained: Crenellation doubles the length of an interface. Thus, a space with a crenellated interface of width $w$ and length $l$ is equivalent to *two* spaces with smooth walls of width $w/2$ and identical length. In other words, we should compare the statistical properties of lignin grown in contact with crenellated hemicellulose in a space of width $w$ with lignin grown between flat walls in a space of width $w/2$. There are three types of sites near a crenellated interface with contact numbers 5, 2, and 1 (Figure 5); each of these occurs equally frequently so the average contact number is $^8/_3$. We therefore predict (based on the arguments above) that, for small to moderate values of $w$, lignin grown near a crenellated interface will have a higher DP and degree of branching and a lower phenyl–OH content than the corresponding state of the flat-interface model (grown in a space of

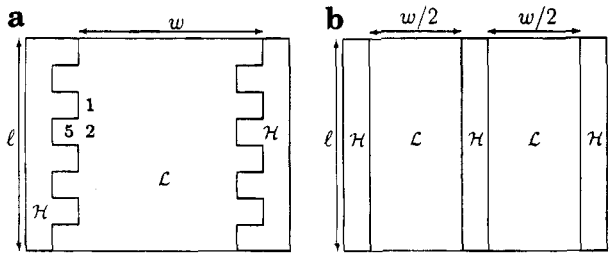


**Figure 5.** (a) Hemicellulose walls with a crenellated interface and (b) smooth hemicellulose walls with an equivalent total interfacial length and simulation area. In both panels, the top and bottom horizontal lines denote the (periodic) boundaries of the simulation plane, $\mathscr{H}$ denotes hemicellulose-occupied space and $\mathscr{L}$ denotes the space available for lignin growth. In panel a, each crenellation occupies one lattice site; the three types of interfacial sites near a crenellation are labeled by their contact numbers.

width $w/2$); at large values of $w$, the two models should give similar results. This is exactly what we observe. Although site exclusion effects are obviously important in two dimensions, they might also be significant in three dimensions, depending on the geometry of the lignin–hemicellulose complex. If there are relatively many lignin–hemicellulose bonds and if typical bonding geometries result in the steric unavailability of many monolignol binding sites, effects similar to those observed above might be found. At least some of the differences between lignins obtained from different parts of the tree might have their origins in hemicellulose interactions.

## 4. Conclusion

Our model reproduces several of the properties of lignin. It is particularly gratifying that the gelation curve and the dependence of the gross properties of the polymer on the rate of monolignol addition correlate so well with experimental data since these properties depend on the dynamics of lignification, which we sought to model. As a result, the structures obtained for this two-dimensional model should bear a close relationship to those found in native lignin.

Despite their importance to lignin biochemistry, lignin–hemicellulose complexes (and other glycolignins) have almost never been modeled, Jurasek's work being the notable exception.[28] Our work demonstrates the importance of the geometry of the hemicellulose matrix. The whole area of lignin–polysaccharide interactions is however worthy of attention. For instance, although bonds between cellulose and lignin have never been observed, the cellulose matrix provides a preferred direction for lignification.[48] Much could be learned from a theoretical study of this effect.

Since a fully realistic model of lignin will require a three-dimensional approach, we are currently studying such generalizations of our methods. In addition, we hope to include in this next-generation model a more complete set of bond types, a more realistic geometric model of the monolignols,[29] and all the features of the current model, including a treatment of hemicellulose.

Dehydrogenative polymerization is an important in vivo macromolecular synthesis pathway.[49] Lignin is only one of many phenolic materials formed in this way: Among others, tannins, terpenoids, and xanthones are also the result of dehydrogenative polymerization. Thus, there is a ready-made set of structural problems which could be addressed with our methods, in addition to the myriad of other macromolecular systems amenable to similar analysis.

**Acknowledgment.** We thank Dr. Lubo Jurasek of Paprican for answering our many questions about lignin and for sharing with us his results prior to publication. We also thank Dr. Dimitris Argyropoulos for drawing to our attention the literature on lignin gelation and Dr. John Schmidt for explaining to us the differences between native and milled wood lignins. This work has been supported by the Protein Engineering Network of Centres of Excellence. M.R.R. was partially supported by an Ontario Graduate Scholarship during the preparation of this work.

## References and Notes

(1) Fengel, D.; Wegener, G. *Wood—Chemistry, Ultrastructure, Reactions*; de Gruyter: Berlin, 1984.
(2) Lindberg, J. J.; Kuusela, T. A.; Levon, K. In *Lignin—Properties and Materials*; Glasser, W. G., Sarkanen, S., Eds.; American Chemical Society: Washington, DC, 1989; pp 190–204.
(3) Struszczyk, H. In *Ligno-cellulosics: Science, Technology, Development and Use*; Kennedy, J. F., Phillips, G. O., Williams, P. A., Eds.; Ellis Horwood: New York, 1992; pp 791–801.
(4) Sjöström, E. *Wood Chemistry—Fundamentals and Applications*, 2nd ed.; Academic: San Diego, CA, 1993.
(5) Goring, D. A. I. In *Lignin—Properties and Materials*; Glasser, W. G., Sarkanen, S., Eds.; American Chemical Society: Washington, DC, 1989; pp 2–10.
(6) Gravitis, J. In *Ligno-cellulosics: Science, Technology, Development and Use*; Kennedy, J. F., Phillips, G. O., Williams, P. A., Eds.; Ellis Horwood: New York, 1992; pp 613–627.
(7) Atalla, R. H.; Agarwal, U. P. *Science* **1985**, *227*, 636–638.
(8) Faulon, J.-L.; Hatcher, P. G. *Energy Fuels* **1994**, *8*, 402–407.
(9) Sarkanen, K. V.; Ludwig, C. H. In *Lignins—Occurrence, Formation, Structure and Reactons*; Sarkanen, K. V., Ludwig, C. H., Eds.; Wiley: New York, 1971; pp 1–18.
(10) Harkin, J. M. In *Oxidative Coupling of Phenols*; Taylor, W. I., Battersby, A. R., Eds.; Dekker: New York, 1967; pp 243–321.
(11) Sarkanen, K. V.; Hergert, H. L. In *Lignins—Occurrence, Formation, Structure and Reactions*; Sarkanen, K. V., Ludwig, C. H., Eds.; Wiley: New York, 1971; pp 43–94.
(12) Glasser, W. G. In *Pulp and Paper—Chemistry and Chemical Technology*, 3rd ed.; Casey, J. P., Ed.; Wiley: New York, 1980; Vol. I, pp 39–111.
(13) Shevchenko, S. M.; Apushkinskii, A. G. *Russ. Chem. Rev.* **1992**, *61*, 105–131.
(14) Forss, K.; Kokkonen, R.; Sågfors, P.-E. In *Lignin—Properties and Materials*; Glasser, W. G., Sarkanen, S., Eds.; American Chemical Society: Washington, DC, 1989; pp 29–41.
(15) Harkin, J. M. *Tappi* **1972**, *55*, 991–996.
(16) Elder, T. In *Lignin—Properties and Materials*; Glasser, W. G., Sarkanen, S., Eds.; American Chemical Society: Washington, DC, 1989; pp 262–271.
(17) Elder, T. In *Viscoelasticity of Biomaterials*; Glasser, W. G., Hatakeyama, H., Eds.; American Chemical Society: Washington, DC, 1992; pp 370–384.
(18) Glasser, W. G.; Glasser, H. R. *Macromolecules* **1974**, *7*, 17–27.
(19) Glasser, W. G.; Glasser, H. R. *Holzforschung* **1974**, *28*, 5–11.
(20) Glasser, W. G.; Glasser, H. R. *Cellulose Chem. Technol.* **1976**, *10*, 23–37.
(21) Glasser, W. G.; Glasser, H. R. *Cellulose Chem. Technol.* **1976**, *10*, 39–52.
(22) Glasser, W. G.; Glasser, H. R.; Nimz, H. H. H. *Macromolecules* **1976**, *9*, 866–867.
(23) Glasser, W. G.; Glasser, H. R.; Morohoshi, N. *Macromolecules* **1981**, *14*, 253–262.
(24) Glasser, W. G.; Glasser, H. R. *Paperi ja Puu* **1981**, *63*, 71–83.
(25) Lange, H.; Wagner, B.; Yan, J. F.; Kaler, E. W.; McCarthy, J. L. *Fourth International Symposium on Wood and Pulping Chemistry*; Paris, 1987; Vol. 1, pp 239–244.
(26) Lange, H.; Wagner, B.; Yan, J. F.; Kaler, E. W.; McCarthy, J. L. *Seventh International Symposium on Wood and Pulping Chemistry*; Beijing, 1993; Vol. 1, pp 111–122.

(27) Bolker, H. I.; Brenner, H. S. *Science* **1970**, *170*, 173–176.
(28) Jurasek, L. *J. Pulp Paper Sci.*, submitted for publication.
(29) Roussel, M. R.; Lim, C. Discrete dynamic polymer model. *J. Comput. Chem.*, submitted for publication.
(30) Haggin, J. *Chem. Eng. News* **1985**, *63* (18), 33–34.
(31) Luner, P.; Kempf, U. *Tappi* **1970**, *53*, 2069–2076.
(32) Toffoli, T.; Margolus, N. *Cellular automata machines*; MIT: Cambridge, MA, 1987.
(33) Meakin, P. *Phys. Rev. Lett.* **1983**, *51*, 1119–1122.
(34) Lai, Y.-T.; Sarkanen, K. V. *Cellulose Chem. Technol.* **1975**, *9*, 239–245.
(35) Grimmett, G. *Percolation*; Springer-Verlag: New York, 1980.
(36) Leclerc, D. F.; Olson, J. A. *Macromolecules* **1992**, *25*, 1667–1675.
(37) Argyropoulos, D. S.; Bolker, H. I. *Macromolecules* **1978**, *20*, 2915–2922.
(38) Argyropoulos, D. S.; Bolker, H. I. *J. Wood Chem. Technol.* **1978**, *7*, 499–512.
(39) Argyropoulos, D. S.; Berry, R. M.; Bolker, H. I. *J. Polym. Sci. B* **1987**, *25*, 1191–1201.
(40) Hall, P. *Introduction to the Theory of Coverage Processes*; Wiley: New York, 1988.
(41) Yang, J.-M.; Goring, D. A. I. *Can. J. Chem.* **1980**, *58*, 2411–2414.
(42) Lai, Y.-Z.; Guo, X.-P.; Situ, W. *J. Wood Chem. Technol.* **1990**, *10*, 365–377.
(43) Francis, R. C.; Lai, Y.-Z.; Dence, C. W.; Alexander, T. C. *Tappi J.* **1991**, *74* (9), 219–224.
(44) Lai, Y.-Z.; Guo, X.-P. *Wood Sci. Technol.* **1991**, *25*, 467–472.
(45) Pan, X.; Lachenal, D.; Lapierre, C.; Monties, B. *J. Wood Chem. Technol.* **1992**, *12*, 135–147.
(46) Argyropoulos, D. S. *Seventh International Symposium on Wood and Pulping Chemistry*; Beijing, 1993; Vol. 2, pp 776–787.
(47) Lai, Y.-Z.; Funaoka, M. *J. Wood Chem. Technol.* **1993**, *13*, 43–57.
(48) Donaldson, L. A. *Wood Sci. Technol.* **1994**, *28*, 111–118.
(49) Taylor, W. I., Battersby, A. R., Eds. *Oxidative Coupling of Phenols*; Dekker: New York, 1967.
(50) Chen, C.-L. In *Wood Structure and Composition*; Lewin, M., Goldstein, I. S., Eds.; Dekker: New York, 1991; pp 183–261.

MA9410126